

## Identification and Characterization of the Genes Responsible for the Production of the Cyclic Lipopeptide Arthrofactin by *Pseudomonas* sp. MIS38

Kenji WASHIO,<sup>1,†</sup> Siew Ping LIM,<sup>2</sup> Niran ROONGSAWANG,<sup>3</sup> and Masaaki MORIKAWA<sup>1</sup>

<sup>1</sup>Division of Biosphere Science, Graduate School of Environmental Science, Hokkaido University, Sapporo 060-0810, Japan

<sup>2</sup>Department of Molecular and Cell Biology, University of California, Berkeley, CA 94720-3202, USA

<sup>3</sup>BIOTEC Central Research Unit, National Center for Genetic Engineering and Biotechnology, Pathumthani 12120, Thailand

Received November 19, 2009; Accepted February 1, 2010; Online Publication, May 7, 2010

[doi:10.1271/bbb.90860]

***Pseudomonas* sp. MIS38 produces an effective biosurfactant named arthrofactin, which is a cyclic lipopeptide synthesized by a mega complex composed of three nonribosomal peptide synthetases. In order to gain insight into the control mechanism of arthrofactin production, a Tn5 mutant library was constructed and screened for arthrofactin-deficient mutants. Along with a number of mutations that occurred in the arthrofactin synthetase operon, three other mutants harbored distinct Tn5 insertions in the genes encoding SyrF-like protein (*arfF*), heat shock protein (*hspG*), and (p)ppGpp synthetase/hydrolase (*spoT*). Epistasis analyses revealed that *spoT* functions early in the arthrofactin production pathway. We also found that *spoT* affects MIS38 swarming, biofilm formation, and the cell morphology.**

**Key words:** arthrofactin; nonribosomal peptide synthetase; (p)ppGpp; *Pseudomonas* sp. MIS38; *spoT*

Many bacteria synthesize complex peptides using a class of multimodular enzymes called nonribosomal peptide synthetase (NRPS).<sup>1</sup> *Pseudomonas* sp. MIS38 is an isolate from oil spills in Japan.<sup>2</sup> This strain produces the cyclic lipopeptide arthrofactin, which contains a head group of seven D- and four L-amino acids linked to a  $\beta$ -hydroxydecanoyl tail (Fig. 1). We have identified an operon encoding arthrofactin synthetase, which is composed of three NRPS subunits (ArfA/B/C).<sup>3</sup> The predicted primary structure of the arthrofactin synthetase subunits follows the co-linearity rule of NRPS, in which 11 sets of iterative catalytic modules are observed. Substrate specificities predicted from the internal 11 modules reflect the order and composition of amino acid residues in the purified arthrofactin.<sup>4</sup> One of the remaining unresolved issues is the occurrence of D-amino acids in the final product. Balibar *et al.* have recently demonstrated a novel type of functional domain embedded in the arthrofactin synthetase, which is responsible for both L- to D-epimerization of amino acids and the formation of a peptide linkage.<sup>5</sup> Hence we hypothesize that a single unit of the three NRPS subunits is sufficient for the basic catalysis of arthrofactin biosynthesis.

Arthrofactin belongs to a group of cyclic lipopeptides from the genus *Pseudomonas* that includes amphisin, tensin, pholipeptin A, and lokisin.<sup>6</sup> The unique structural features of cyclic lipopeptides allow these molecules to function as antibiotics, immunosuppressants, antitumor agents, siderophores, and surfactants.<sup>1</sup> Despite their potential industrial and pharmaceutical significance, the natural roles of cyclic lipopeptides are poorly understood. A previous study of ours showed that the amphiphilic properties of arthrofactin are superior in acting as a pivotal biosurfactant like surfactin from *Bacillus subtilis*.<sup>4</sup> The absence of arthrofactin production impairs swarming and biofilm formation,<sup>3</sup> suggesting an indispensable role of arthrofactin in the social behavior of MIS38.

Because cyclic lipopeptides are required for the ecological fitness of bacteria, their production is exquisitely modulated by environmental stimuli and intracellular signals.<sup>7</sup> To determine how arthrofactin production is controlled by MIS38, we employed transposon 5 (Tn5)-based mutagenesis and identified the genes responsible for arthrofactin production.

### Materials and Methods

**Bacterial strains and growth conditions.** *Pseudomonas* sp. MIS38 was previously isolated from oil spills in Shizuoka Prefecture, in central Japan.<sup>2</sup> The *arfB::kan* mutant impaired in one of the arthrofactin synthetases was generated by insertion of the kanamycin (*kan*) gene cassette in *arfB*.<sup>3</sup> *Escherichia coli* NovaBlue (Novagen, Madison, WI) was used as host strain for the general cloning of DNA fragments. Cloning vector pBluescript II SK<sup>+</sup> (Stratagene, La Jolla, CA) and pGEM-T EASY (Promega, Madison, WI) were used in *E. coli*. Expression vector pME6032 was used for the complementation test.<sup>8</sup>

MIS38 and the mutant strains were grown in Luria-Bertani (LB) liquid medium at 30 °C with shaking at 150 rpm. For swarming assay, 1  $\mu$ l of the culture (OD<sub>600</sub> = 0.5) was placed at the center of a 0.7% LB agar plate and incubated at 30 °C for 12 h. The swarming area was determined by measuring the diameter of the swarmed area.

**Screening of arthrofactin-deficient mutants.** *E. coli* SM10  $\lambda$ -pir carrying pUTmini-Tn5 Km (Biomedal, Seville, Spain) was used for the conjugative transfer of mini-Tn5 transposon. pUTmini-Tn5 Km was transferred from SM10  $\lambda$ -pir to MIS38 cells by conjugation on a 1.5% LB agar plate at 30 °C for 16 h. After conjugation, the cells were recovered in 10 mM MgSO<sub>4</sub> and spread onto a 1.5% LB agar plate containing 30  $\mu$ g/ml of kan and 10  $\mu$ g/ml of chloramphenicol (chl), so

<sup>†</sup> To whom correspondence should be addressed. Fax: +81-11-706-2281; E-mail: washi@ees.hokudai.ac.jp

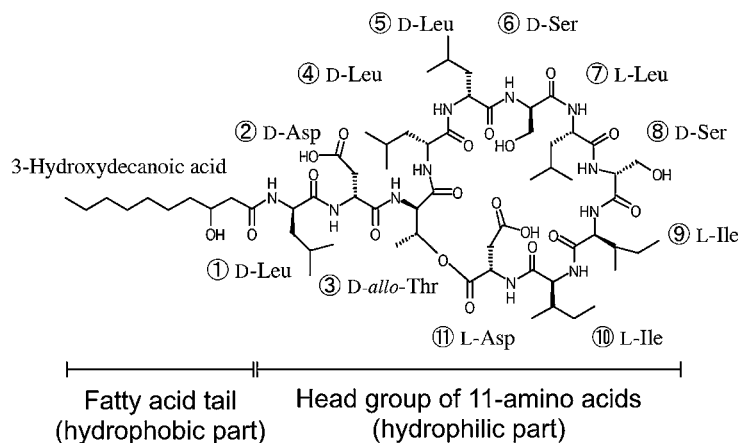


**Fig. 1.** Chemical Structure of Arthrofactin.

Arthrofactin consists of a hydrophilic head group of an 11-amino acid cyclic peptide linked to a hydrophobic  $\beta$ -hydroxydecanoyl tail.

that growth of the wild-type MIS38 ( $kan^s$ ,  $chl^r$ ) and *E. coli* SM10  $\lambda$ -pir ( $kan^r$ ,  $chl^s$ ) might be arrested. Transconjugants ( $kan^r$ ,  $chl^r$ ) that exhibited morphological characters similar to those of the *arfB::kan* mutant,<sup>3</sup> without halo formation on a 1.5% LB agar plate overlaid with crude oil, were selected as candidates. After initial screening, the arthrofactin production of each mutant was estimated by oil displacement activities in the culture supernatant.<sup>4</sup>

**General DNA manipulations.** For inverse PCR, chromosomal DNA was digested with *Pst* I and self-ligated by standard methods.<sup>9</sup> The self-ligated DNAs were used as template for inverse PCR in combination with two primers complementary to the internal sequences of mini-Tn5 (Table 1). PCR products were gel-purified using the QIAquick Gel Extraction Kit as described in the manufacturer's protocol (Qiagen, Hilden, Germany). The nucleotide sequences of the PCR fragments were determined by BigDye terminator cycle sequencing on an ABI model 3100 DNA sequencer (Perkin-Elmer Applied Biosystems, Wellesley, MA). Flanking regions near the target gene were amplified by chromosome walking PCR and their nucleotide sequences were determined. Sequence data have been submitted to the public database under accession nos, AB107223 (*arfA/B/C* and *arfF*), AB262445 (*htpG*), and AB262446 (*spoT*).

The copy numbers of the Tn5 insertion were estimated by Southern blot analysis with the *Pst* I-digested genomic DNAs of the Tn5 mutants. The 510-bp fragment of the *kan* gene in Tn5 (nucleotide positions, 511–1,020 in pME6032) was obtained by PCR, labeled with alkaline phosphatase, and used as probe in Southern hybridization (Fig. 2B). Hybridized bands were visualized by an AlkPhos Direct Labelling and Detection System (GE Healthcare, Waukesha, WI).

**HPLC analysis of arthrofactin production.** MIS38 and the mutant strains were grown in LB medium at 30 °C for 2 d. Bacterial cells were removed by centrifugation repeated once ( $10,000 \times g$  for 15 min) at 4 °C. Hydrophobic fractions containing arthrofactin were precipitated at 4 °C, by acidification of the supernatant to pH 2.0 with 6 N HCl. The precipitates were extracted with 100% methanol. The extract containing arthrofactin was diluted to a 10% methanol solution, and a portion (200  $\mu$ l) was subjected to reverse phase HPLC analysis, as described previously (HP1100) (Hewlett Packard, Chicago, IL).<sup>3</sup>

**Construction of expression plasmids.** The gene fragments of *arfF*, *htpG*, and *spoT* were amplified by PCR from the MIS38 DNA using the various sets of primers spanning the entire coding region (Table 1). The PCR fragment was blunt-ended with a DNA blunting kit (Takara Bio, Shiga, Japan), digested with *Sac* I (underlined in Table 1), and cloned between *Sac* I and the blunt-ended *Pst* I sites in pME6032 ( $Tet^r$ ). The resulting plasmids, pArF6032;  $P_{tac}::arfF$  (1–264 aa), pHtpG6032;  $P_{tac}::htpG$  (1–634 aa), and pSpoT6032;  $P_{tac}::spoT$  (1–701 aa), were introduced into MIS38 and the Tn5 mutant cells by electroporation. In pME6032, the exogenous gene was inducible with addition of isopropyl thiogalactopyranoside (IPTG). Transformants

were grown in LB medium containing 12.5  $\mu$ g/ml of tetracycline and 1 mM IPTG.

**Reverse transcriptase (RT) PCR.** Total RNA was extracted from bacterial cells using the RNeasy Mini Kit (Qiagen). cDNA was synthesized from 1  $\mu$ g of DNase-treated RNA as described previously.<sup>10</sup> PCR amplification was performed using the various sets of primers for the target gene (Table 1) and Ex Taq DNA polymerase (Takara Bio). PCR condition was 3 min at 94 °C, followed by 35 (*spoT*) or 30 (except for *spoT*) cycles of 30 s at 94 °C, 30 s at 58 °C and 30 s at 72 °C, and 5 min at 72 °C. The PCR products were run on 1.5% agarose gel in  $1 \times$  TBE (89 mM Tris-borate, 2 mM EDTA) and visualized by ethidium bromide staining. 16S rRNA was used as an internal control to normalize the amount of templates.

**Biofilm formation.** Biofilm formation in a polypropylene tube was tested as described previously.<sup>11</sup> After standing cultivation in a 1.5-ml microcentrifuge tube (TC131615) (Nippon Genetics, Tokyo) containing 300  $\mu$ l of LB medium at 20 °C, the surface of the biofilms was rinsed with distilled water and stained with 500  $\mu$ l of 0.1% (w/v) crystal violet (CV) solution for 25 min. The CV solution was removed and the tube was washed twice with distilled water. The CV attached to the biofilm was dissolved in 400  $\mu$ l of 95% ethanol, and quantified by measuring its absorbance at 590 nm.

**ppGpp analysis.** Nucleotides were extracted with formic acid.<sup>12</sup> Bacterial cells were recovered from LB liquid culture at 30 °C for 2 d by centrifugation and suspended in distilled water ( $OD_{600} = 2.0$ ). Five ml of this suspension was transferred into a 50-ml polypropylene tube containing 0.5 ml of 11 M formic acid, then vigorously mixed and incubated on ice for 30 min. These samples were centrifuged at  $10,000 \times g$  for 10 min at 4 °C. The supernatant was filtered through 0.2- $\mu$ m filters and stored at –20 °C until use in HPLC analysis.

The sample of 200  $\mu$ l was separated by ion pair reverse phase HPLC using a Cosmosil 5C<sub>18</sub> AR II column (4.6  $\times$  150 mm) (Nakalai Tesque, Kyoto, Japan) at a flow rate of 1.0 ml/min. The mobile phase consisted of 125 mM KH<sub>2</sub>PO<sub>4</sub>, 10 mM tetrabutyl ammonium dihydrogen phosphate, 60 ml/l methanol, and 1 g/l KOH (pH 6.0).<sup>13</sup> The eluted nucleotides were monitored by the sample absorbance at 254 nm and identified by comparison with the retention time of authentic standards. ppGpp standard was purchased from a company (TriLink Biosciences, San Diego, CA).

**Scanning electron microscopy.** Biofilms grown in a 1.5-ml polypropylene tube at 20 °C for 3 d were rinsed with distilled water, fixed with 5% OsO<sub>4</sub>, and postfixed with 2% glutaraldehyde in 0.1 M phosphate-buffered saline (pH 7.0). The fixed samples were then dehydrated through a series of graded ethanol solutions, critical point dried, and then coated with gold-palladium under high vacuum. They were observed with a Model S-2400 scanning electron microscope (SEM) (Hitachi, Tokyo).

**Table 1.** Oligonucleotide Primers Used in the Experiments

Oligonucleotide primers for the inverse PCR of the MIS38 DNA				
Gene	Forward primer		Reverse primer	
mini-Tn5 transposon	mTn5_f	5'-AAGGTGATCCGGTGGATGAC-3'	mTn5_r	5'-CAATCGGCTGCTCTGATGCCGC-3'
Oligonucleotide primers for the <i>kan</i> probe fragment on Southern blot analysis				
Gene	Forward primer		Reverse primer	
<i>kan</i>	kan_f	5'-ACGCTGCCCAAGCATCAGG-3'	kan_r	5'-CCGGACAGGTCGGTCTTGAC-3'
Oligonucleotide primers for the RT-PCR analysis				
Gene	Forward primer		Reverse primer	
<i>arfB</i>	arfB_f	5'-GGCAAACCTCGACCGCAAGGC-3'	arfB_r	5'-GGCGTAGCCTGCCAAGGTCG-3'
<i>arfF</i>	arfF_f	5'-TCGTGGAACACCTGCTGCAA-3'	arfF_r	5'-GTCGCTCCAGCCGCAACATC-3'
<i>htpG</i>	htpG_f	5'-GCTGCTGCACCTCATGATCC-3'	htpG_r	5'-AATCGGCGGTGCCCGACTTG-3'
<i>spoT</i>	spoT_f	5'-TCGGCGAAGGCGAACAGCTG-3'	spoT_r	5'-TTCCAGCTCGACGCGCAGCT-3'
16S rRNA	16S_f	5'-ACGGGTGAGTAATGCCTAGG-3'	16S_r	5'-CAGGCTTTGCCCATTTGTCC-3'
Oligonucleotide primers for the complementation test with pME6032				
Gene	Forward primer		Reverse primer	
<i>arfF</i>	arfF_Extf	5'-ACGAGCTCATGAATCTGACCGGCAGCAT-3'	arfF_Ext_r	5'-CCCTCGAGTTATGCCCCAGCCATCCAGC-3'
<i>htpG</i>	htpG_Extf	5'-GGGAGCTCATGACCATGAGTGTGGAAAC-3'	htpG_Ext_r	5'-CAGGTACCTCAAGCTGACAGTTCAACCA-3'
<i>spoT</i>	spoT_Extf	5'-GCGGGAGCTCAGCCTACGGCAGGAG-3'	spoT_Ext_r	5'-GGGGTACCTTAGGCACGCATGCGGGTGA-3'

## Results

### Identification of arthrofactin-deficient mutants

A mutant library of MIS38 was generated by conjugal transfer of mini-Tn5. Since arthrofactin is a dominant extracellular biosurfactant produced by MIS38, we obtained 24 candidate arthrofactin-deficient mutants from approximately 20,000 transconjugants based on the characteristics of the *arfB::kan* mutant,<sup>3)</sup> which impairs oil displacement activity in the culture supernatant (Table 2). Nucleotide sequencing of the genes flanking the Tn5 insertion sites revealed that most of the mutations (21 of 24) occurred in the arthrofactin synthetase operon. The mutants could be divided into three other classes based on distinct Tn5 insertions in the genes for *arfF* (encoding SyrF-like protein), *htpG* (heat shock protein 90), and *spoT* ((p)ppGpp synthetase/hydrolase) in the forward orientation (Fig. 2A). Southern blot analysis using a probe for the *kan* gene in Tn5 revealed that there was a single Tn5 insertion in each of the three mutants (Fig. 2B). We designated these mutants *arfF::Tn5*, *htpG::Tn5*, and *spoT::Tn5*, and used them in further experiments.

The *arfF* gene is adjacent to the 5' terminus of the *arfA/B/C* operon, in an opposite orientation. The deduced amino acid sequence of ArfF (264 residues) shares high identity with that of SyrF-like proteins in *P. fluorescence* PfO-1 (identity 85%, accession no. ABA73953), *P. fluorescence* Pf-5 (63%, AAY91417), and *P. syringae* pv. *syringae* B301D (48%, AAK83330). HtpG is a prokaryotic homolog of eukaryotic heat shock protein 90 (HSP90), and MIS38 HtpG is composed of 634 residues with a predicted molecular size of 71.2 kDa. This protein shows 59% identity with the *E. coli* Hsp90.<sup>14)</sup> The SpoT protein in MIS38 (701 residues, 78.6 kDa) has 54% identity with *E. coli* SpoT.<sup>15)</sup> SpoT is a bifunctional enzyme responsible for the hydrolysis of

**Table 2.** Summary of the Arthrofactin-Deficient Mutants Obtained by Mini-Tn5 Mutagenesis

Integrated gene	Lengths of ORF (bp)	Gene product (aa)	Insertion site*	Overlapping clones							
<i>arfA</i>	6,414 bp	arthrofactin synthetase, ArfA (2,137 aa)	1,049 bp	1							
			2,524 bp	4							
			2,529 bp	2							
			5,058 bp	17							
			5,083 bp	5							
<i>arfB</i>	13,017 bp	arthrofactin synthetase, ArfB (4,338 aa)	1,325 bp	1							
			4,437 bp	2							
			4,442 bp	1							
			12,834 bp	1							
<i>arfC</i>	17,775 bp	arthrofactin synthetase, ArfC (5,924 aa)	614 bp	2							
			1,603 bp	3							
			2,099 bp	4							
			5,043 bp	2							
			5,658 bp	1							
			10,526 bp	3							
			10,793 bp	2							
			11,077 bp	2							
			11,831 bp	3							
<i>arfF</i>	795 bp	SyrF-like protein (264 aa)	549 bp	1							
			<i>htpG</i>	1,905 bp	heat shock protein 90 (634 aa)	133 bp	1				
						<i>spoT</i>	2,106 bp	(p)ppGpp synthetase/hydrolase (701 aa)	1,663 bp	3	
									Total candidates		65

\*Insertion site of the mini-Tn5 transposon is numbered by the position (bp) starting from adenine of the tentative translation initiation codon ATG.

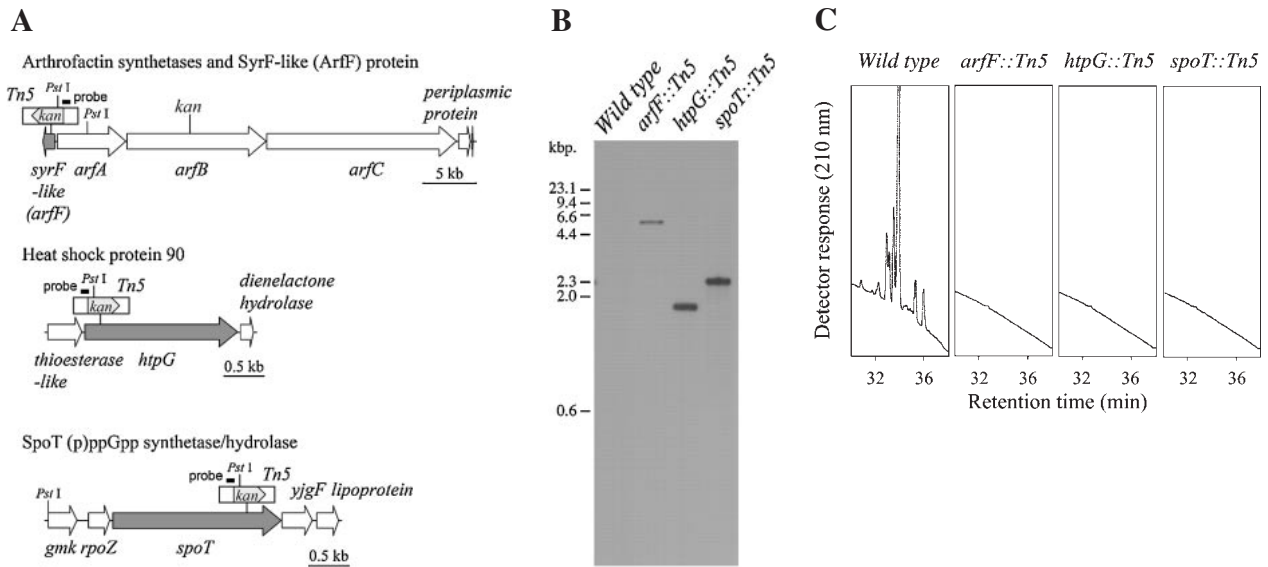


**Fig. 2.** The Tn5 Mutagenesis of MIS38.

A, Gene organization of MIS38. Arrows indicate the direction of transcription. Upper arrows show positions of the Tn5 insertion (*Tn5*) including the kanamycin resistant gene (*kan*). The *kan* gene cassette used in gene disruption of *arfB* is indicated.<sup>3)</sup> Protein coding regions, carrying the Tn5 insertion, are shaded. The region used as probe for Southern blot analysis is indicated by a bold line in Tn5 (probe). Restriction sites for *Pst* I adjacent to Tn5 are also shown. B, Southern blot analysis to estimate the copy numbers of Tn5 integrated into the genome DNA (*arfF::Tn5*, *htpG::Tn5*, and *spoT::Tn5*). C, HPLC analysis of arthrofactin production in the wild-type and the Tn5 mutants. Methanol soluble fractions were prepared from 2-d cultures of the wild-type, *arfF::Tn5*, *htpG::Tn5*, and *spoT::Tn5* mutants. Chromatograms were obtained by detection at a wavelength of 210 nm.

guanosine 3', 5'-bispyrophosphate (ppGpp) and the synthesis of guanosine 3'-diphosphate 5'-triphosphate (pppGpp). ppGpp and pppGpp, collectively called (p)ppGpp, is a key regulator of the stringent response and also acts in secondary metabolism.<sup>16)</sup>

#### Arthrofactin production in the Tn5 mutants

When HPLC chromatograms from the wild-type and mutant strains were compared, the major peaks corresponding to the arthrofactin fractions were not seen in the three mutants (Fig. 2C). To confirm that the absence of arthrofactin production was caused by Tn5-mediated gene inactivation, we complemented each Tn5 mutant with a pME6032 plasmid carrying the intact *arfF* (pArfF6032), *htpG* (pHtpG6032), and *spoT* (pSpoT6032) (Fig. 3A). The vector control had no effect on arthrofactin production in the wild-type or the mutant strain. Arthrofactin production by the *arfF::Tn5* and *htpG::Tn5* mutants was fully or partially restored by complementation with pArfF6032 and pHtpG6032 respectively. However, pSpoT6032 failed to rescue arthrofactin production of the *spoT::Tn5* mutant. These data suggest that *arfF* and *htpG* are necessary for normal arthrofactin production. The failure of complementation of the *spoT::Tn5* mutant raises the possibility that the Tn5 insertion modified the function of *spoT* or caused polar effects on neighboring genes.

To confirm the results of the complementation tests, we conducted RT-PCR on RNA samples prepared from 1-d cultures of the wild-type and mutant strains (Fig. 3B). The expression of the arthrofactin synthetase gene cluster was monitored by *arfB*, because the *arfA/B/C* genes are co-transcribed to produce a single mRNA.<sup>17)</sup> Expression levels of *arfB* markedly decreased in the *arfF::Tn5* and *spoT::Tn5* mutants, whereas no significant change was observed in the *htpG::Tn5*

mutant. When each Tn5 mutant was complemented by the plasmid vector designated to express the wild-type gene (Fig. 3B), the transcript levels of *arfB* were fully restored in the *arfF::Tn5* mutant carrying pArfF6032. On the other hand, *arfB* expression was not restored in the *spoT::Tn5* mutant carrying pSpoT6032. The reason for this is currently unclear.

#### Epistasis analysis of the genes responsible for arthrofactin production

The wild-type and arthrofactin-deficient strains exhibited similar growth curves when grown in LB liquid culture (Fig. 4A). To investigate functional linkages among the identified genes, we compared their transcript levels during the growth of the MIS38 and mutant strains (Fig. 4B). In the wild type, the transcript levels of *arfB* were considerably elevated during the transition from the exponential to the stationary phase (8–12 h). Transcript levels of *arfF* were essentially constant throughout the growth phases, but increased transiently just prior to the induction of *arfB* (4–8 h). This parallelism suggests a direct role of ArfF in the transcription of *arfA/B/C*. The expression patterns of *htpG* and *spoT* were antagonized with those of *arfB*. The reciprocal expression observed between *htpG*, *spoT*, and the arthrofactin synthetase gene cause the complexities of arthrofactin production, which is controlled positively or negatively by the growth periods.

We also compared the expression patterns of the genes identified in each mutant (Fig. 4B). The transcript levels of *arfB* decreased markedly in the *arfF::Tn5* mutant. In the *htpG::Tn5* mutant, the levels of the regulatory (*arfF*, *spoT*) and synthetase genes (*arfB*) did not change. These results also support the idea that *arfF* positively controls transcription of the arthrofactin synthetase gene and that *htpG* acts in post-

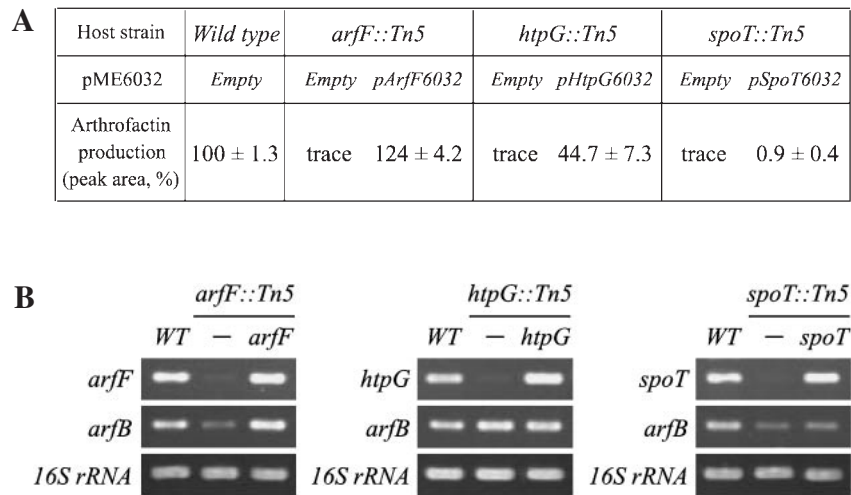


**Fig. 3.** Complementation Test of the Tn5 Mutants.

A, Arthrofactin production of the plasmid-harboring strain, estimated by the peak area of HPLC analysis. Combinations of the host strain and plasmid DNAs (pArfF6032, pHtpG6032, and pSpoT6032) are indicated in parentheses. Methanol soluble fractions, including arthrofactin, were prepared from culture supernatants grown in LB liquid culture at 30 °C for 2 d. The experiment was repeated 3 times, and the average value is shown. The errors indicate the standard errors of the means. B, RT-PCR analyses showing restored levels of *arfF*, *htpG*, *spoT*, and *arfB* expression in the Tn5 mutants. RNA samples were prepared from bacterial cells grown in LB liquid culture at 30 °C for 1 d.

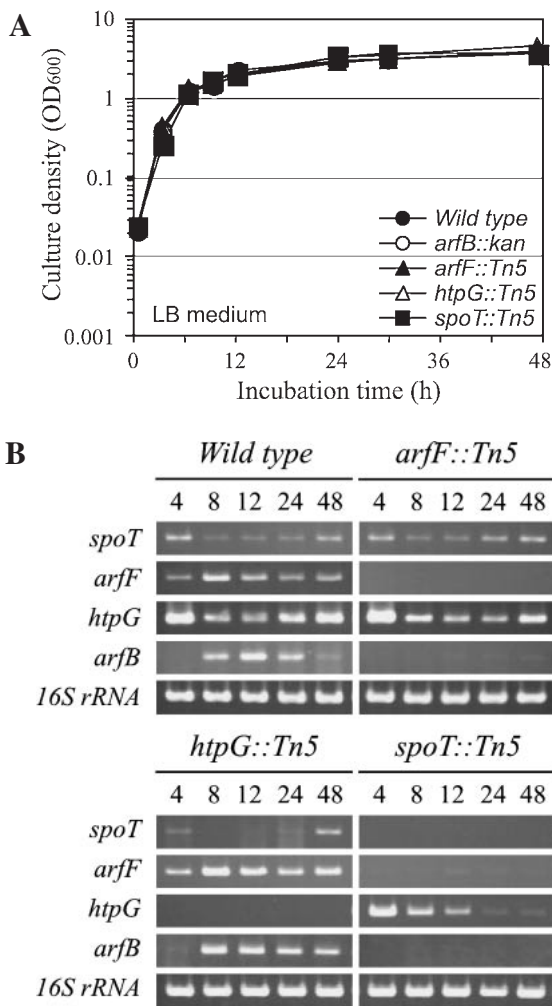


**Fig. 4.** RT-PCR Analysis of the Genes Responsible for Arthrofactin Production.

Total RNA was extracted from the wild type and the Tn5 mutants (*arfF::Tn5*, *htpG::Tn5*, and *spoT::Tn5*) grown in LB liquid culture for different times (4, 8, 12, 24, and 48 h) and subjected to RT-PCR with the various sets of primers for the target gene (Table 1).

transcriptional processes leading to the production of arthrofactin. In the *spoT::Tn5* mutant, the levels of *arfB* and *arfF* transcripts were significantly decreased over the growth phase, whereas *htpG* transcripts were lower only in the later stationary phase. The observation in the *spoT::Tn5* mutant implies that *spoT* plays more crucial roles in the arthrofactin biosynthesis pathway than the other regulatory genes.

#### Physiological characterization of the Tn5 mutants

The phenotypes of the three mutants were characterized by assaying swarming and biofilm formation (Fig. 5). The wild type swarmed over the plate to cover an area of 14.5 cm<sup>2</sup>. The swarmed areas of the *arfF::Tn5*, *htpG::Tn5*, and *spoT::Tn5* mutants were only 2.0, 4.2, and 0.28 cm<sup>2</sup> respectively (Fig. 5A). The *spoT::Tn5* cells did not spread, indicating a complete loss of swarming ability. Although all the mutants were deficient in arthrofactin production, their swarming abilities were distinct. This confirms that swarming is a complex social behavior influenced by many gene functions that cannot be explained simply by the production of arthrofactin.

Biofilm formation was measured by the crystal violet staining method.<sup>11)</sup> During 1 d of culture in a 1.5-ml polypropylene tube, the wild type formed a thick biofilm at the air/medium interface that was stable for 1 d (Fig. 5B). Biofilm formation by MIS38 decreased drastically after 2 d, perhaps due to cell detachment from the biofilm. The *arfF::Tn5* and *htpG::Tn5* mutants formed a more extensive biofilm than the wild type after 1 d, and declined afterwards. Several explanations have been proposed for the roles of cyclic lipopeptides in biofilm formation. The cell surface hydrophobicity conferred by amphiphilic properties facilitates the contact of cells with a solid surface and enhances biofilm formation,<sup>18)</sup> or surfactant activities inhibit cell adhesion and break down biofilms.<sup>19)</sup> Since the *arfF::Tn5* and *htpG::Tn5* mutants, which are defective in arthrofactin production, detached from the biofilm,

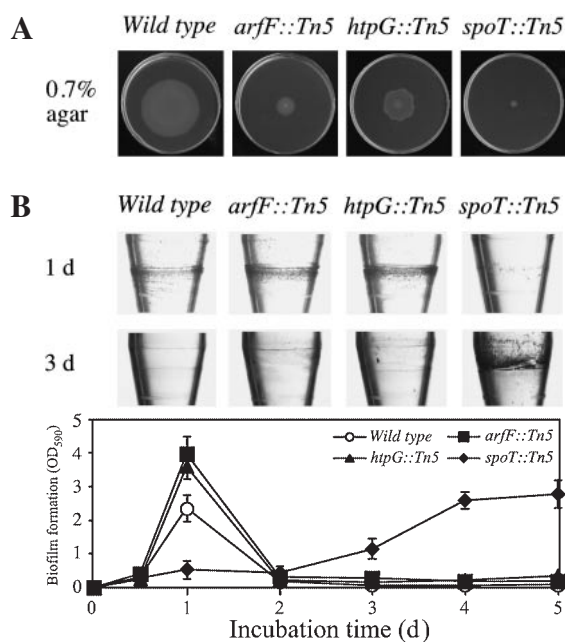


**Fig. 5.** Physiological Characterizations of the Tn5 Mutants.

A, Swarming patterns in the wild type and the Tn5 mutants. Swarming assay was performed at 30°C on a 0.7% agar LB plate. The area of swarming migration was assessed in triplicate. B, Biofilm formation of the wild type and the Tn5 mutants. After incubation for 1 or 3 d, the area of the biofilm ring was stained with 0.1% crystal violet (CV) solution and observed by light microscopy. The CV attached to biofilms was dissolved in 95% ethanol, and was quantified by measuring its absorbance at 590 nm. All data are averages of triplicate experiments. The error bars indicate standard errors of the means.

dispersal of the biofilm appears to be independent of arthrorfactin production.

The *spoT::Tn5* mutant formed fewer biofilms after 1 d, but longer incubation significantly stimulated biofilm formation. We do not know whether this was due to stimulation of cell adhesion or prevention of cell dispersal. SEM observation showed that a small number of the wild-type cells had attached at 3 d, whereas the *spoT::Tn5* cells grew into aggregates and exhibited robust biofilms (Fig. 6). Notably, the *spoT::Tn5* mutant produced large amounts of extracellular matrix and was tethered by a fibrous network. This finding indicates that the drastic changes in cell surface properties occurred due to the *spoT::Tn5* mutation and resulted in a distinct sessile morphotype.

#### *ppGpp* production in the *spoT::Tn5* mutant

Previous analysis has indicated that basal levels of (p)ppGpp increase in the *spoT* mutants due to a lack of (p)ppGpp degradation, and thus most phenotypes observed in the *spoT* mutants were likely due to over-production of (p)ppGpp.<sup>20</sup> Based on this, we monitored the cellular levels of ppGpp in the wild type and the *spoT::Tn5* mutant (Fig. 7). In our assay system, ppGpp levels were below the detectable range in the wild type after 2 d, whereas the accumulation of ppGpp increased in the *spoT::Tn5* mutant. This suggests that the *spoT::Tn5* mutation results in over-pooling of ppGpp such that the arthrorfactin production pathways is inhibited by the negative effects of ppGpp.

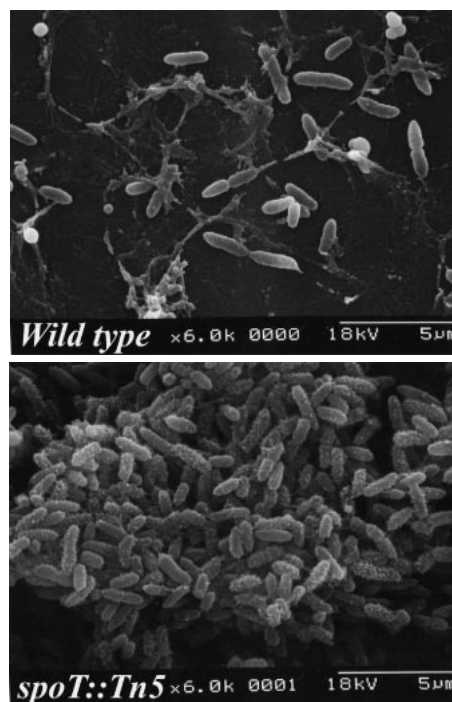


**Fig. 6.** SEM Observation of the Wild-Type and the *SpoT::Tn5* Biofilm Cells.

Biofilms of the wild type and the *spoT::Tn5* mutant were developed in LB medium kept standing at 20°C for 3 d.

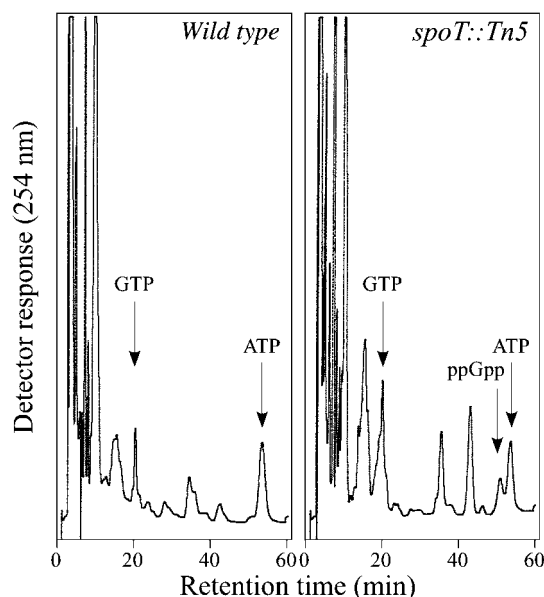


**Fig. 7.** ppGpp Production in the Wild Type and the *SpoT::Tn5* Mutant.

Cellular levels of ppGpp were monitored by ion pair reverse phase HPLC analysis. The positions of authentic standards are indicated by arrows (GTP, ppGpp, and ATP). ppGpp is eluted at 56 min under these current conditions. The peaks of GTP and unknown nucleotides in the *spoT::Tn5* mutant also increased in parallel with the accumulation of ppGpp. A link between ppGpp production and changes of cellular GTP pool has been postulated.<sup>27,34</sup>

## Discussion

In this study, we isolated and characterized MIS38 mutants that do not produce arthrorfactin. We found that Tn5 insertions into *arfF*, *htpG*, and *spoT* substantially reduced arthrorfactin production. ArfF is a LuxR-type

transcription factor<sup>21</sup>) and an evident homolog of SyrF.<sup>22</sup>) The *syrF* and *salA* genes for the LuxR-family proteins locate in the NRPS operon, responsible for the production of two lipopeptides, syringomycin and syringopeptin, in *P. syringae* pv. *syringae* B301D. SyrF transactivated the target NRPS promoter *via* the trans-activation of SalA.<sup>22</sup>) Genome surveys of *P. fluorescence* PfO-1 and Pf-5, which are close relatives of MIS38,<sup>17</sup>) indicated similar gene organization of *syrF* homologs located upstream of the putative NRPS genes for arthrofactin-like cyclic lipopeptides, suggesting conserved roles of SyrF-like proteins among related *Pseudomonas* spp.<sup>6</sup>)

Unlike transcriptional control by ArfF, normal expression of the genes for arthrofactin production was retained in the *htpG::Tn5* mutant (Fig. 4B). We do not know how HtpG is involved in arthrofactin biosynthesis. However, previous studies indicate that mutations in the gene encoding DnaK, a HSP70 class heat shock protein, prevent *Pseudomonas putida* PCL1445 from producing two cyclic lipopeptides, putisolvin I and II.<sup>23</sup>) The same report revealed that the role of DnaK, together with DnaJ, is to regulate expression of the putisolvin synthetase genes. Thus the *in vivo* role of molecular chaperones may be to ensure proper folding of positive transcription factors or synthetic machinery. Bacterial HtpG lacks an extension of the C-terminal domain, which serves as the major interaction site with co-chaperones in eukaryotes, and appears to have tasks distinct from eukaryotic HSP90.<sup>24</sup>) A role of HtpG in the proper assembly of multimodular enzymes has been proposed for the polyketide albicidin synthetase in *Xanthomonas albilineans*.<sup>25</sup>)

Our study showed that the cellular levels of ppGpp were unusually elevated in the *spoT::Tn5* mutant, abrogating arthrofactin production (Fig. 7). Bacteria are known to produce (p)ppGpp in response to nutritional starvation, which triggers a stringent response resulting in growth arrest or induction of stress tolerance.<sup>16</sup>) Previous studies have revealed that proper levels of (p)ppGpp are required for antibiotic production by *Streptomyces*.<sup>26,27</sup>) Natural roles of cyclic peptides have been proposed to yield ecological advantages for bacteria, such as creating a protective microenvironment by reducing surface tension, nutrient uptake, or facilitating swarming to move to a more favorable environment.<sup>6</sup>) Our studies indicated that arthrofactin production is closely linked with the communal behavior of MIS38, including swarming and biofilm formation.<sup>3</sup>) These natural traits are very important for the ecological fitness of bacteria, and it is logical that arthrofactin production is governed by the SpoT-dependent (p)ppGpp regulon.

In general, Gram-negative bacteria have a set of enzymes, RelA and SpoT, responsible for the metabolism of (p)ppGpp.<sup>28</sup>) RelA mainly contributes to the synthesis of (p)ppGpp during amino acid starvation, while SpoT is a bifunctional enzyme that can hydrolyze or synthesize (p)ppGpp in response to various types of starvation and stress *via* unknown mechanisms.<sup>29</sup>) In the complete absence of *spoT*, basal levels of (p)ppGpp gradually increased due to the remaining activity of *relA*, and consequently caused growth arrest for lethality.<sup>20,30</sup>) This means that *spoT* is essential for most

Gram-negative bacteria. To our surprise, the MIS38 *spoT::Tn5* mutant was not lethal and did not exhibit growth arrest (Fig. 3). To recapitulate the *spoT::Tn5* mutation, we cloned a DNA fragment flanking *spoT* in suicide vector pCVD442<sup>31</sup>) and attempted to remove *spoT* by homologous recombination. However, we failed to obtain complete *spoT* null alleles (data not shown). The preliminary data indicate an essential role of *spoT* in MIS38 and raise the question why the *spoT::Tn5* mutant of MIS38 grows normally.

A Pfam database search (<http://pfam.sanger.ac.uk/>) predicted that MIS38 SpoT contains multiple domains, including the N-terminal catalytic domains for the metabolism of (p)ppGpp and the C-terminal TGS and ACT regulatory domains. It is notable that the *spoT::Tn5* mutant contained a Tn5 insertion near the 3' terminus of *spoT* (Fig. 2A), leaving a normal 5' gene region that encodes the N-terminal catalytic domain. When the transcript species derived from *spoT* were analyzed by RT-PCR with different primers used in Fig. 4, expression of the 5' region of *spoT* was further retained in the *spoT::Tn5* mutant (data not shown). Therefore, the *spoT::Tn5* mutant may produce a truncated version of SpoT with altered activities. This idea is strengthened by the fact that forced expression of distinct segments of SpoT homologous proteins has a variety of effects on (p)ppGpp metabolism.<sup>32,33</sup>) To confirm this, we are currently performing *in vivo* gene manipulation of *spoT* in MIS38, with the goal of explaining the link between SpoT function and arthrofactin production.

## Acknowledgments

*E. coli* SM10  $\lambda$ -pir and pCVD442 were kindly supplied by Dr. D. A. Hogan (Dartmouth Medical School, NH) and Dr. R. Kolter (Harvard Medical School, MA). This work was supported by the New Energy and Industrial Technology Development Organization (NEDO), the Institute for Fermentation of Osaka (IFO), and a Grant-in-Aid for Scientific Research from the Japan Society for the Promotion of Science (JSPS, to MM).

## References

- Schwarzer D, Finking R, and Marahiel MA, *Nat. Prod. Rep.*, **20**, 275–287 (2003).
- Morikawa M, Daido H, Takao T, Murata S, Shimonishi Y, and Imanaka T, *J. Bacteriol.*, **175**, 6459–6466 (1993).
- Roongsawang N, Hase K, Haruki M, Imanaka T, Morikawa M, and Kanaya S, *Chem. Biol.*, **10**, 869–880 (2003).
- Morikawa M, Hirata Y, and Imanaka T, *Biochim. Biophys. Acta*, **1488**, 211–218 (2000).
- Balibar CJ, Vaillancourt FH, and Walsh CT, *Chem. Biol.*, **12**, 1189–1200 (2005).
- Raaijmakers JM, de Bruijn I, and de Kock MJ, *Mol. Plant Microbe Interact.*, **19**, 699–710 (2006).
- Dubern JF and Bloemberg GV, *FEMS Microbiol. Lett.*, **263**, 169–175 (2006).
- Heeb S, Itoh Y, Nishijyo T, Schnider U, Keel C, Wade J, Walsh U, O'Gara F, and Haas D, *Mol. Plant Microbe Interact.*, **13**, 232–237 (2000).
- Sambrook J and Russell DW, "Molecular Cloning, a Laboratory Manual" 3rd ed., Cold Spring Harbor Laboratory Press, Cold Spring Harbor (2001).
- Takei D, Washio K, and Morikawa M, *Biotechnol. Lett.*, **30**, 1447–1452 (2008).

- 11) Iijima S, Washio K, Okahara R, and Morikawa M, *Microb. Biotech.*, **2**, 361–369 (2009).
- 12) Traxler MF, Summers SM, Nguyen HT, Zacharia VM, Hightower GA, Smith JT, and Conway T, *Mol. Microbiol.*, **68**, 1128–1148 (2008).
- 13) Funabashi H, Mie M, Yanagida Y, Kobatake E, and Aizawa M, *Biotechnol. Lett.*, **24**, 269–273 (2002).
- 14) Bardwell JC and Craig EA, *Proc. Natl. Acad. Sci. USA*, **84**, 5177–5181 (1987).
- 15) Sarubbi E, Rudd KE, Xiao H, Ikehara K, Kalman M, and Cashel M, *J. Biol. Chem.*, **264**, 15074–15082 (1989).
- 16) Potrykus K and Cashel M, *Annu. Rev. Microbiol.*, **62**, 35–51 (2008).
- 17) Lim SP, Roongsawang N, Washio K, and Morikawa M, *J. Appl. Microbiol.*, **107**, 157–166 (2009).
- 18) Pamp SJ and Tolker-Nielsen T, *J. Bacteriol.*, **189**, 2531–2539 (2007).
- 19) Kuiper I, Lagendijk EL, Pickford R, Derrick JP, Lamers GE, Thomas-Oates JE, Lugtenberg BJ, and Bloemberg GV, *Mol. Microbiol.*, **51**, 97–113 (2004).
- 20) Murray KD and Bremer H, *J. Mol. Biol.*, **259**, 41–57 (1996).
- 21) de Bruijn I and Raaijmakers JM, *Appl. Environ. Microbiol.*, **75**, 4753–4761 (2009).
- 22) Wang N, Lu SE, Records AR, and Gross DC, *J. Bacteriol.*, **188**, 3290–3298 (2006).
- 23) Dubern JF, Lagendijk EL, Lugtenberg BJ, and Bloemberg GV, *J. Bacteriol.*, **187**, 5967–5976 (2005).
- 24) Wandinger SK, Richter K, and Buchner J, *J. Biol. Chem.*, **283**, 18473–18477 (2008).
- 25) Vivien E, Megessier S, Pieretti I, Cociancich S, Frutos R, Gabriel DW, Rott PC, and Royer M, *FEMS Microbiol. Lett.*, **251**, 81–89 (2005).
- 26) Hesketh A, Sun J, and Bibb M, *Mol. Microbiol.*, **39**, 136–144 (2001).
- 27) Gomez-Escribano JP, Martín JF, Hesketh A, Bibb MJ, and Liras P, *Microbiology*, **154**, 744–755 (2008).
- 28) Battesti A and Bouveret E, *J. Bacteriol.*, **191**, 616–624 (2009).
- 29) Srivatsan A and Wang JD, *Curr. Opin. Microbiol.*, **11**, 100–105 (2008).
- 30) Xiao H, Kalman M, Ikehara K, Zemel S, Glaser G, and Cashel M, *J. Biol. Chem.*, **266**, 5980–5990 (1991).
- 31) Donnenberg MS and Kaper JB, *Infect. Immun.*, **59**, 4310–4317 (1991).
- 32) Mechold U, Murphy H, Brown L, and Cashel M, *J. Bacteriol.*, **184**, 2878–2888 (2002).
- 33) Avarbock A, Avarbock D, Teh JS, Buckstein M, Wang ZM, and Rubin H, *Biochemistry*, **44**, 9913–9923 (2005).
- 34) Ochi K, *J. Gen. Microbiol.*, **132**, 2621–2631 (1986).